

# ENGINEERING PROCESS MODEL FOR HIGH-TEMPERATURE ELECTROLYSIS SYSTEM PERFORMANCE EVALUATION

*Carl M. Stoots, James E. O'Brien, Michael G. McKellar, Grant. L. Hawkes  
Idaho National Laboratory  
2525 N. Fremont Ave., Idaho Falls, ID, 83415, USA*

## ABSTRACT

In order to evaluate the potential hydrogen production performance of large-scale High-Temperature Electrolysis (HTE) operations, the INL has developed an engineering process model using the commercial systems-analysis code HYSYS. Using this code, a detailed process flowsheet has been defined that includes all the components that would be present in an actual plant such as pumps, compressors, heat exchangers, turbines, and the electrolyzer. Since the electrolyzer is not a standard HYSYS component, a custom one-dimensional electrolyzer model was developed for incorporation into the overall HYSYS process flowsheet. This electrolyzer model allows for determination of operating voltage, gas outlet temperatures, and electrolyzer efficiency for any specified inlet gas flow rates, current density, cell active area, and external heat loss or gain. The one-dimensional electrolyzer model was validated by comparison with results obtained from a fully 3-D computational fluid dynamics model developed using FLUENT. This report provides details on the one-dimensional electrolyzer model, the HYSYS process model for a 300 MW HTE plant, and some representative results of parametric studies performed using the HYSYS process model.

## INTRODUCTION

A research program is under way at the Idaho National Laboratory (INL) to assess the performance of solid-oxide cells operating in the steam electrolysis mode for hydrogen production over a temperature range of 800 to 900°C. The research program includes both experimental and modeling activities. Experimental activities, including both single button-cell testing and stack testing, have been documented in several recent publications [e.g., 1-3]. The modeling activities include detailed computational fluid dynamics (CFD) simulations [4,5] and system-level process modeling.

System-level engineering process modeling was undertaken to evaluate the potential hydrogen-production performance of large-scale high-temperature electrolysis (HTE) operations. This model was developed at the INL using the commercial system-analysis code HYSYS. Using this code, several detailed process flow sheets have been defined that include all of the components that would be present in an actual HTE plant such as pumps, compressors, heat exchangers, turbines, and the electrolyzer. Since the high-temperature electrolyzer unit is not a standard HYSYS component, a custom one-dimensional electrolyzer model was developed for incorporation into the overall process flow sheet. This electrolyzer model allows for the determination of the average Nernst potential, cell operating voltage, gas outlet temperatures, and electrolyzer efficiency for any specified inlet steam, hydrogen, and sweep-gas flow rates, current density, cell active area, and external heat loss or gain. The one-dimensional electrolyzer model was validated by comparison with results obtained from a fully 3-D computational fluid dynamics model and by comparison with experimental results. These comparisons may be found in [6]. This report provides details on the one-dimensional electrolyzer model, the HYSYS process model for a 300 MW HTE plant, and some

representative results of parametric studies performed using HYSYS with the custom electrolyzer model.

## ELECTROLYZER MODEL FOR SYSTEM ANALYSIS

In general, for an operating electrolysis stack, there will be a temperature change associated with the electrolysis process. For these cases, the energy equation for electrolysis process can be written as:

$$\dot{Q} - \dot{W} = \sum_P \dot{N}_i [\Delta H_{f_i}^o + H_i(T_P) - H_i^o] - \sum_R \dot{N}_i [\Delta H_{f_i}^o + H_i(T_R) - H_i^o] \quad (1)$$

where  $\dot{Q}$  is the external heat transfer rate to or from the electrolyzer,  $\dot{W}$  is the rate of electrical work supplied to the electrolyzer,  $\dot{N}_i$  is the molar flow rate of each reactant or product,  $\Delta H_{f_i}^o$  is the standard-state enthalpy of formation of each reactant or product and  $H_i(T) - H_i^o$  is the sensible enthalpy for each reactant or product. Applying the energy equation in this form, all reacting and non-reacting species included in the inlet and outlet streams can be accounted for, including inert gases, inlet hydrogen (introduced to maintain reducing conditions on the steam/hydrogen electrode), and any excess unreacted steam. Determination of the outlet temperature from Eqn. (1) is an iterative process. The heat transferred during the process must first be specified (e.g., zero for the adiabatic case). The temperature-dependent enthalpy values of all species must be available from curve fits or some other data base. The solution procedure begins with specification of the cathode-side inlet flow rates of steam, hydrogen, and any inert carrier gas such as nitrogen (if applicable). The inlet flow rate of the sweep gas (e.g., air or steam) on the anode side must also be specified. Specification of the gas flow rates allows for the determination of the inlet mole fractions of steam, hydrogen, and oxygen that appear in the Nernst equation. The steam mole fraction is expressed in terms of the hydrogen mole fraction as  $1 - y_{H_2} - y_{N_2}$ .

The current density and active cell area are then specified, yielding the total operating current. Care must be taken to insure that the specified inlet gas flow rates and total cell current are compatible. The minimum required inlet steam molar flow rate is the same as the steam consumption rate, given by:

$$\dot{N}_{i,H_2O,\min} = \Delta \dot{N}_{H_2O} = \frac{I}{2F} N_{cells} = \frac{i A_{cell}}{2F} N_{cells} = \Delta \dot{N}_{H_2} \quad (2)$$

which is of course also equal to the hydrogen production rate.

Once the total and per-cell hydrogen production rates are known, the outlet flow rates of hydrogen and steam on the cathode side and oxygen on the anode side can be determined. The flow rates of any inert gases, the anode-side sweep gas, and any excess steam or hydrogen are the same at the inlet and the outlet. Once all these flow rates are known, the summations in Eqn. (1) can be evaluated. The product summation must be evaluated initially at a guessed value of the product temperature,  $T_P$ .

The operating voltage corresponding to the specified current density is obtained from:

$$V_{op} = \bar{V}_{Nernst} + i \times ASR(T) \quad (3)$$

where the stack area-specific resistance,  $ASR(T)$ , must be estimated and specified as a function of temperature. The cell-mean Nernst potential can then be obtained from an integrated Nernst equation:

$$\bar{V}_{Nernst} = \frac{1}{2F(T_P - T_R)(y_{o,O_2,A} - y_{i,O_2,A})(y_{o,H_2,C} - y_{i,H_2,C})} \times \int_{T_R}^{T_P} \int_{y_{i,O_2,A}}^{y_{o,O_2,A}} \int_{y_{i,H_2,C}}^{y_{o,H_2,C}} \Delta G_R(T) - RT \ln \left( \frac{1 - y_{H_2} - y_{N_2}}{y_{H_2} y_{O_2}^{1/2}} \right) dy_{H_2} dy_{O_2} dT \quad (4)$$

where  $y_{i,O_2,A}$  is the anode-side inlet mole fraction of oxygen, etc. Note that the upper limit of integration on the temperature integral,  $T_P$ , is initially unknown. Once the  $ASR$  and the mean Nernst potential are known, the operating voltage is obtained from Eqn. (3) and the electrical work term in Eqn. (1) is obtained from  $\dot{W} = -V_{op}I$ . An algorithm then must be developed to iteratively solve for the product temperature,  $T_P$ , in order to satisfy Eqn. (1). This algorithm can then be imbedded in a loop so that a full numerical “sweep” can be performed. We have implemented this procedure in MathCad. The MathCad model provides accurate estimates of electrolyzer operating voltage (and corresponding electrolyzer efficiency) and outlet temperatures, for any specified electrolyzer heat loss or gain, gas flow rates, current density, and per-cell  $ASR(T)$ . This electrolyzer model was developed for incorporation into system-level electrolysis plant models being developed using HYSYS system simulation software. With a realistic electrolyzer model incorporated into the overall HYSYS plant model, good estimates of overall hydrogen-production efficiencies can be obtained over a wide range of prospective operating conditions.

Representative results obtained from the integral electrolyzer model for an adiabatic case are presented in Figs. 1 and 2, along with results obtained from FLUENT. A more comprehensive comparison may be found in [6]. Fig. 1 shows predicted voltage-current characteristics and Fig. 2 shows predicted gas outlet temperatures. The 1-D integral model predicts somewhat higher operating voltages compared to the FLUENT results. This makes the 1-D model conservative since higher operating voltages correspond to lower electrolysis efficiencies. Note that, for an operating voltage near the thermal minimum (~1.06 V), both models predict outlet temperatures for this particular adiabatic case that are about 30°C lower than the inlet temperatures. Per-cell gas flow rates for this case were based on the flow rates used in recent planar HTE stack tests [1, 2]. The 1-D model also predicts the correct value of the thermal neutral voltage for 800°C, 1.287 V. At this operating voltage, the outlet temperatures are equal to the inlet temperatures under adiabatic conditions. The 1-D model is also useful for assessing the effect of using a steam sweep rather than an air sweep on the oxygen side. Use of a sweep gas that does not contain oxygen is advantageous because it reduces the Nernst potential, thereby increasing the electrolysis efficiency for a specified current density. We are considering the use of steam for the sweep gas since it would be relatively easy to separate the steam from the produced oxygen by condensation. The produced oxygen then can be sold as a commodity. Incorporation of the 1-D model into our HYSYS system simulation will enable a broad range of parametric studies.

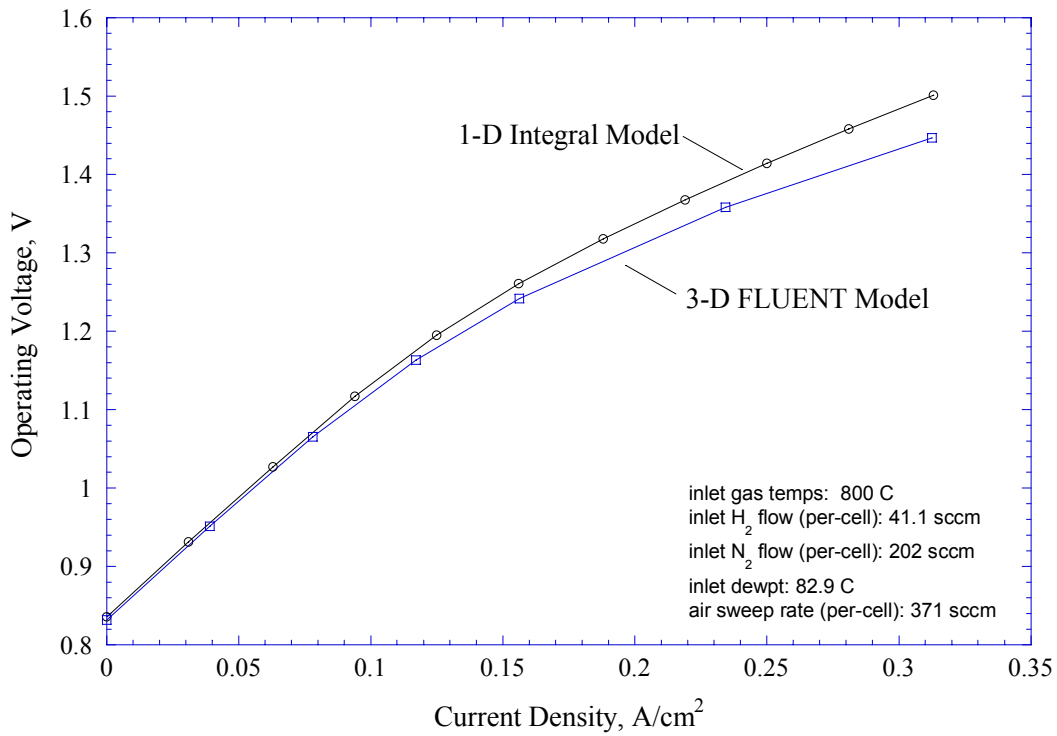


Figure 1. Operating voltage as a function of current density for adiabatic electrolyzer operation, predicted from a 1-D integral model and from a full 3-D FLUENT simulation.

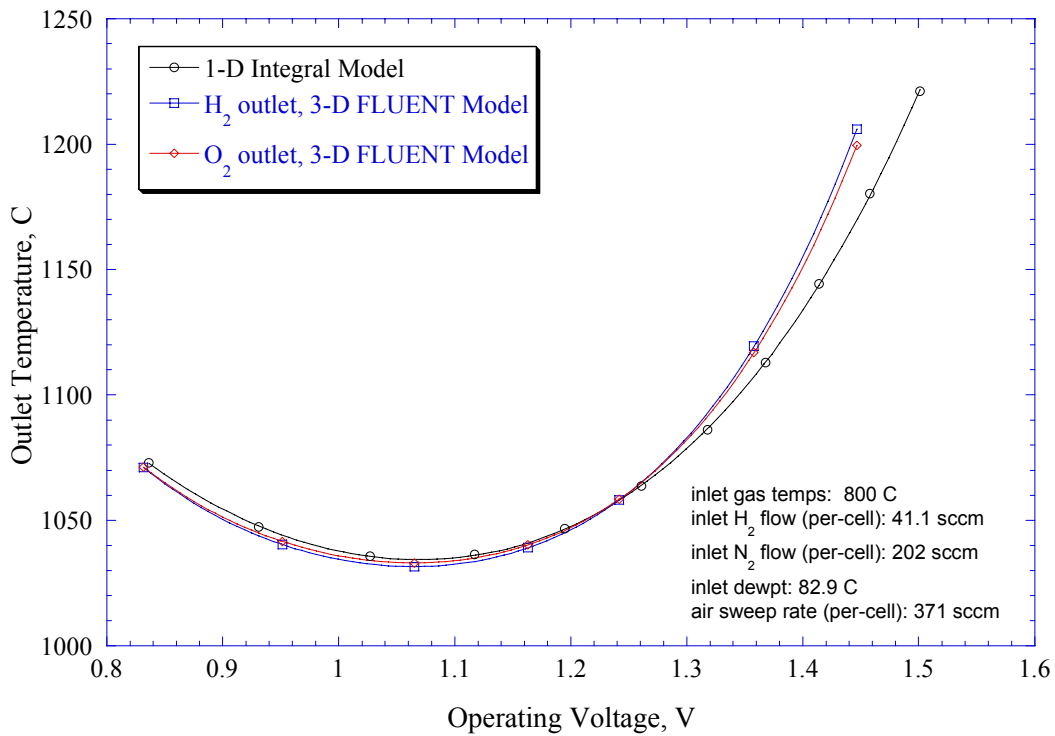


Figure 2. Predicted gas outlet temperatures for adiabatic electrolyzer operation; comparison of 1-D integral MathCad model with full 3-D FLUENT simulation.

## OVERALL PROCESS THERMAL-TO-HYDROGEN EFFICIENCY

In order to assess the overall hydrogen production efficiency of a large-scale HTE process, the entire process must be defined, including all of the important components that will be required. The feedstock for any large-scale HTE process will be liquid water at ambient temperature and pressure, and the products will be hydrogen and oxygen, ultimately also at ambient temperature. The HTE process may occur at elevated pressure, so the products may also be delivered at elevated pressure. In order to maximize the overall process efficiency, it is essential to recuperate as much of the process heat as possible.

To compare the performance of the HTE process to alternate hydrogen production techniques, we have adopted a general efficiency definition that can be applied to any thermal water-splitting process, including HTE, low-temperature electrolysis (LTE), and thermochemical processes. Since the primary energy input to the thermochemical processes is in the form of heat, the appropriate general efficiency definition to be applied to all of the techniques is the overall thermal-to-hydrogen efficiency,  $\eta_H$ . This efficiency is defined as the heating value of the produced hydrogen divided by the total thermal input required to produce it. Either the low heating value, LHV, or the high heating value, HHV, of the hydrogen can be used. From a process efficiency viewpoint, since the feedstock is liquid water, it makes sense to use the high heating value. From a utilization viewpoint, depending on the application, it may make more sense to use the low heating value. We will use the low-heating-value definition in this report:

$$\eta_H = \frac{LHV}{\sum_i Q_i}. \quad (5)$$

The denominator in this efficiency definition quantifies all of the net thermal energy that is consumed in the process. For a thermochemical process, this summation includes the direct nuclear process heat as well as the thermal equivalent of any electrically driven components such as pumps, compressors, etc. The thermal equivalent of any electrical power consumed in the process is the power divided by the thermal efficiency of the power cycle. We are using an assumed power-cycle thermal efficiency of 45% for the comparisons made in this paper. An advanced power cycle driven by a high-temperature nuclear reactor should easily be able to achieve this thermal efficiency value [7]. For an electrolysis process, the summation in the denominator of Eqn. (5) includes the thermal equivalent of the primary electrical energy input to the electrolyzer and the secondary contributions from smaller components such as pumps and compressors. In addition, any direct thermal inputs are also included. Direct thermal inputs include any net (not recuperated) heat required to heat the process streams up to the electrolyzer operating temperature and any direct heating of the electrolyzer itself required for isothermal operation.

## HYSYS MODEL

We are using HYSYS process-modeling software to evaluate the overall performance of a large-scale HTE plant. The HYSYS model provides process conditions (T, P), mixture compositions, and flow rates for the various flow streams at the numbered locations shown in Figs. 3, 5 and 6. It also provides compressor and heater power requirements, and heat exchanger sizing (UA) information. Three different HYSYS process flow diagrams were

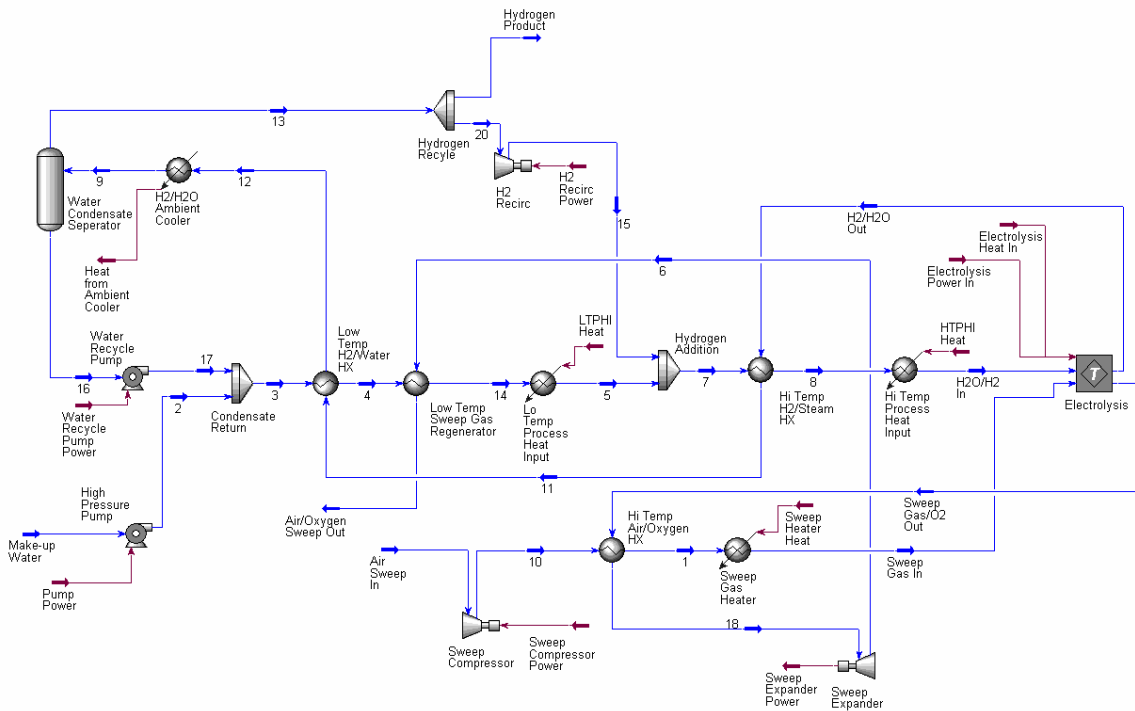


Figure 3. HYSYS process flow diagram for a 300 MW HTE plant with air sweep.

developed for this study, corresponding to the three different oxygen-side sweep conditions that were considered: air sweep, steam sweep, and no sweep. The HYSYS process flow diagram that was developed for the air-sweep case is shown in Fig. 3. In the diagram, the liquid or gas flow streams are shown in blue. Power and heat inputs are shown in red/brown. The HTE plant model has been designed to recover as much heat from the outlet streams as possible. Nevertheless, due to the relative heat capacity rates of the product gas streams and the liquid water inlet stream, net heat addition will always be required to supply at least some of the enthalpy of vaporization of the liquid water and to boost the electrolyzer inlet stream (steam/hydrogen) to the desired stack inlet temperature (800-850°C). In a full-scale plant the net heat for the low- and high-temperature heaters would ideally be supplied as process heat from the reactor, assuming the reactor outlet temperature is high enough. Heat of vaporization can be supplied at relatively low temperature, whereas the final temperature boost to the stack operating temperature will require high-temperature nuclear process heat. For an HTE plant, it may be possible to take advantage of power-cycle waste-heat rejection to preheat the liquid water feedstock. This strategy would directly boost the overall hydrogen-production efficiency since this waste heat input would not have to be included in the denominator of Eqn. (5). This possibility will be considered in future studies.

Referring to Fig. 3, the process feedstock (make-up) water enters in the bottom left. The water is pumped to the process operating pressure in the liquid phase (stream #2). We have evaluated system operation at both atmospheric pressure and at 5 MPa. This make-up stream is combined with water condensate returned from the hydrogen/steam product stream (stream #17) to produce stream #3. The water then enters the low-temperature steam/hydrogen heat exchanger designed to preheat the water to at least the saturated liquid state (265°C at 5 MPa). This is a recuperating heat exchanger that extracts heat from the

outlet hydrogen/steam gas stream. This heat exchanger also serves to condense some of the steam from the hydrogen/steam outlet gas mixture, lowering the dewpoint temperature of that stream to near ambient. Additional heat recuperation from the outlet air/oxygen stream is accomplished in the low-temperature sweep gas regenerator.

External net heat addition required to fully vaporize the inlet H<sub>2</sub>O is supplied by the low-temperature process heater. As the name implies, this heat can be supplied at relatively low-temperature, which improves the second-law efficiency of the process. The efficiency definition given in Eqn. (5) is strictly a first-law efficiency. Downstream of this heater, the steam is mixed with sufficient hydrogen to yield a gas mixture of at least 5% hydrogen and 95% steam, on a molar (or volume) basis. Although not required thermodynamically, the hydrogen helps to maintain reducing conditions at the electrolysis stack cathode, to prevent oxidation of the nickel cermet material. Note that the hydrogen is recycled from the electrolyzer outlet stream, using a small recirculation compressor. The compressor, which will operate at 5 MPa is required to overcome the various pressure drops in the system. A mass-flow controller can be used to regulate the flow rate of the hydrogen to achieve the desired inlet mixture composition of 5 – 10% hydrogen by volume.

Downstream of the hydrogen addition tee, the gas mixture is sent through a high-temperature heat exchanger. This heat exchanger recuperates high-temperature heat from the hot hydrogen/steam electrolyzer-outlet gas. This heat exchanger is designed to preheat the inlet steam/hydrogen gas stream to as close to the desired electrolyzer operating temperature as is practical. Before entering the stack, the gas inlet stream passes through the high-temperature process heater to boost the gas mixture to the stack inlet temperature. A baseline stack operating temperature of 827°C (1100 K) has been used in our performance analyses. The effect of varying this operating temperature has also been examined.

Downstream of the high-temperature process heater, the steam/hydrogen mixture enters the electrolyzer, which has been incorporated directly into HYSYS as a module that is based on the 1-D model described previously. The HYSYS electrolyzer module includes two inlet streams, one for steam/hydrogen and the other for a sweep gas. Possible sweep conditions considered in this study include air sweep, steam sweep, and no sweep. The electrolyzer module also includes an input for the electrolyzer power and an input for direct heat addition. Any value of heat addition can be input to the model. The primary heat addition cases of interest are adiabatic and isothermal. Zero heat addition corresponds to adiabatic cases. Since there is no sensible enthalpy change for the isothermal case, the magnitude of the heat transfer required to achieve isothermal operation,  $\dot{Q}(T)$ , can be calculated directly from the following form of the first law:

$$\dot{Q}(T) = \Delta \dot{N}_{H_2} \Delta H_R(T) - I V_{op} \quad (6)$$

and since the hydrogen production rate,  $\Delta \dot{N}_{H_2}$  is equal to  $I/2F$ , and the thermal neutral voltage,  $V_{tn} = \Delta H_R(T)/2F$ ,

$$\dot{Q}(T) = I(V_{tn} - V_{op}). \quad (7)$$

Note that this result predicts positive heat transfer to the electrolyzer for operating voltages less than thermal neutral and negative heat transfer (i.e., heat rejection from the electrolyzer) for operating voltages greater than thermal neutral.

The outlet streams leave the electrolyzer at a temperature that is dependent on the total flow rate, the amount of heat addition (e.g., isothermal or adiabatic electrolysis) to the electrolyzer, and the operating voltage (e.g., see Fig. 2). The operating voltage also has a significant effect on the electrolysis efficiency. We can derive an expression for the hydrogen production efficiency as a function of the operating voltage for an electrolysis process. For a control volume drawn **only** around the electrolysis stack, with  $W_e=VI$ , inlet and outlet streams at  $T, P$ , direct application of the first law and the definition of the overall thermal-to-hydrogen efficiency with the numerator expressed as the enthalpy of reaction at the operating temperature,  $\Delta H_R$  yields an expression for the electrolyzer overall thermal-to-hydrogen efficiency:

$$\eta_T = \frac{\Delta H_R}{2FV_{op}(1/\eta_P - 1) + \Delta H_R} \quad (8)$$

Therefore lower operating voltages always yield higher efficiencies. Low operating voltages can be achieved in practice, with reasonable current densities, only if the electrolyzer area-specific resistance is low. Note that at  $V_{op} = V_{tn}$ , Eqn. (8) yields  $\eta_T = \eta_P$ . Operation at the thermal neutral voltage yields the same overall hydrogen production efficiency as that of the power cycle. Letting  $V_{op} = E_o = \Delta G_R/2F$ , Eqn. (8) yields

$$\eta_{T,E_o} = \frac{\Delta H_R}{\Delta G_R(1/\eta_P - 1) + \Delta H_R} \quad (9)$$

which is the electrolyzer overall efficiency corresponding to operation at the reference open-cell potential,  $E_o$ . This value is always higher than the power-production thermal efficiency. The open-cell potential corresponding to the electrolyzer operating conditions, including temperature and gas partial pressures, is given by the Nernst equation:

$$E_{oc} = E_o - \frac{R_u T}{jF} \ln \left[ \left( \frac{y_{H_2O}}{y_{H_2} y_{O_2}^{1/2}} \right) \left( \frac{P}{P_{std}} \right)^{-1/2} \right] \quad (10)$$

For a specified temperature, the open-cell potential can be significantly lower than  $E_o$  for high steam mole fraction, low hydrogen mole fraction, low oxygen mole fraction, and low operating pressure. For electrolysis, it is desirable to have as low of a Nernst potential as possible, since the operating cell current density is proportional to the difference between the operating voltage and the Nernst potential. If the Nernst potential is low, a reasonable current density can be achieved with a low operating voltage, and therefore with high efficiency, according to Eqn. (8). The effect of operating potential on the electrolyzer overall thermal-to-hydrogen efficiency is illustrated in Fig. 4. This figure shows a series of overall efficiency curves, over a range of assumed power-production efficiency values for an electrolysis temperature of 800°C. Note that operating at any voltage lower than thermal neutral yields a hydrogen-production efficiency that is greater than the power-cycle thermal efficiency. On the steam/hydrogen side of the electrolysis cell, the use of high inlet steam mole fraction and a high total steam flow rate is desirable, subject to the constraint that a hydrogen content of 5 –

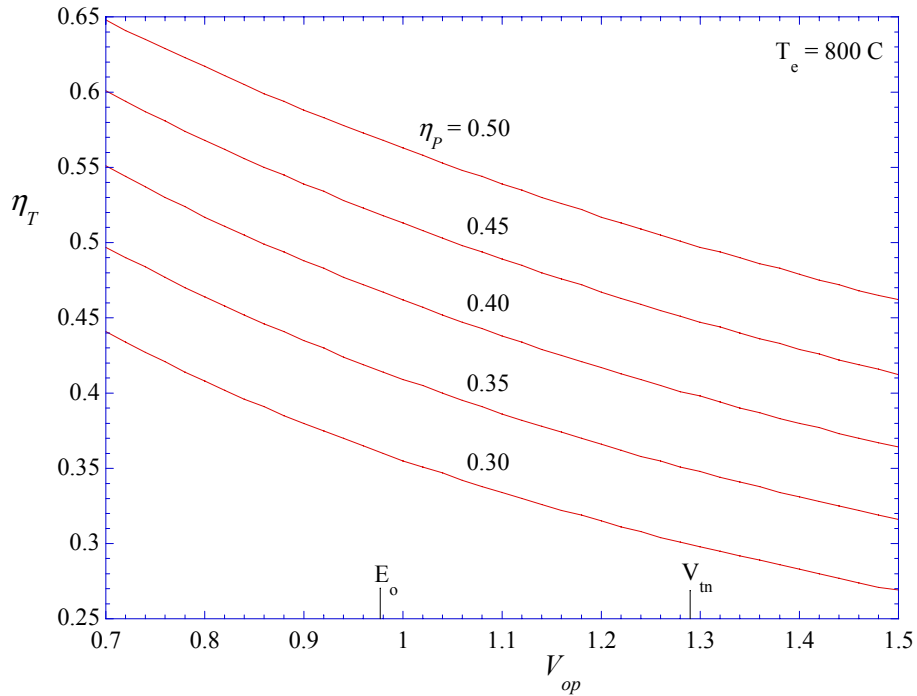


Figure 4. Electrolyzer overall hydrogen production efficiencies as a function of power-production thermal efficiency and electrolyzer per-cell operating voltage.

10% must be used in order to maintain reducing conditions on the steam/hydrogen electrode. On the oxygen side, a low average oxygen mole fraction is desirable. Therefore, a non-oxygen-containing sweep gas should be considered with a high flow rate. This is why we are considering the use of steam as a sweep gas on the oxygen side of these cells. The steam can be separated from the oxygen later by a heat-recuperating condensation process, yielding a pure oxygen product at low temperature.

As an example HTE operating condition, assume  $T = 800^{\circ}\text{C}$ ,  $P = 1 \text{ atm}$ ,  $y_{\text{H}_2\text{O}} = 0.95$ ,  $y_{\text{H}_2} = 0.05$ ,  $y_{\text{O}_2} = 0.05$ ,  $\text{ASR} = 0.5 \text{ Ohm cm}^2$ , and  $\eta_P = 0.45$ . Under these conditions, the Nernst potential is 0.772 V. If we wish to achieve a current density of  $0.25 \text{ A/cm}^2$ , the required operating voltage would be 0.897 V, yielding an electrolyzer hydrogen production efficiency of 0.54 for the assumed power-production efficiency of 0.45. So, with favorable operating conditions, high-temperature electrolysis can yield overall hydrogen-production efficiencies that are significantly higher than the power-cycle thermal efficiency. Furthermore, if the electrolysis process is powered by a high-efficiency advanced reactor/power cycle, overall thermal-to-hydrogen efficiencies greater than 50% can be achieved.

Current electrical production power cycle efficiencies are around 35%. Conventional low-temperature electrolysis, due to higher open-cell potentials and higher overpotentials, displays per-cell operating voltages in the 1.6 – 1.7 range, yielding overall thermal-to-hydrogen-production efficiencies of less than 35%.

It should be emphasized that this discussion of electrolyzer overall thermal-to-hydrogen efficiency based on Eqn. (8) and Fig. 4 does not consider the entire HTE system. The control volume for this discussion is drawn only around the electrolyzer and the inlet and

outlet streams are assumed to be at the same high temperature (i.e., isothermal operation). No consideration of heatup of the process streams to the electrolyzer temperature is included, so these efficiency values are optimistic. Nevertheless, this analysis provides guidance for optimizing the performance of the electrolyzer itself.

Returning to the discussion of the HYSYS system model, the hydrogen/steam outlet stream leaves the electrolyzer and passes through the high- and low-temperature heat exchangers for heat recuperation to the inlet stream. At station 12 in Fig. 3, a low-temperature ambient cooler has been placed in the system. This cooler is needed in some cases in order to insure that a high enough percentage of the steam is condensed out of the hydrogen product stream. Steam content at station 13 should be less than 1%. The condensate is recycled back into the main liquid water inlet flow at station 17. A small water recycle pump (station 16) is required to overcome the various pressure losses through the system.

Sweep gas enters the system and is immediately sent through the sweep compressor to bring it up to system pressure, consuming significant sweep compressor power in the process. This compressor also heats the inlet air significantly. At station 10, the sweep gas enters a heat exchanger to recuperate heat directly from the hot electrolyzer-outlet air/oxygen gas mixture. An additional sweep gas heater is required for the final temperature boost to bring the gas up to the desired electrolyzer inlet temperature. Downstream of the electrolyzer, the sweep gas is sent through the high-temperature air/oxygen heat exchanger and is then expanded through a turboexpander to recover some of the power required to compress the sweep gas in the first place. Finally, the air/oxygen sweep gas is sent through the low-temperature sweep gas regenerator heat exchanger before being exhausted to the surroundings.

A HYSYS process flow diagram that was developed for the steam-sweep case is shown in Fig. 5. It is similar to the air-sweep case, but some reconfiguration of the recuperating heat exchangers was necessary in order to achieve better overall heat recovery from the process streams. This case is complicated by the possibility of phase change on both the steam/hydrogen side and on the sweep side. This factor can lead to temperature pinch problems in the heat exchangers. On the steam/hydrogen side, the major difference between this flow diagram and the air-sweep case occurs at station 12, downstream of the low-temperature H<sub>2</sub>/water recuperating heat exchanger, where the hydrogen/steam product stream is sent to another recuperating heat exchanger (heat regenerator 2) to help preheat the steam sweep inlet line.

On the sweep side, for this case, the sweep stream enters the system as ambient-temperature and ambient-pressure liquid water. The water is compressed to the system operating pressure in the liquid phase, and then preheated by regenerator 1 from the low-temperature end of the sweep gas outlet line and by regenerator 2 from the hydrogen/steam outlet line. The preheated liquid water is partially vaporized at the high-temperature O<sub>2</sub>/steam heat exchanger. Complete vaporization and final temperature boost to the electrolyzer inlet temperature is provided by net high-temperature process heat addition at the sweep gas heater. Downstream of the electrolyzer, the sweep gas is sent through the high-temperature O<sub>2</sub>/steam heat exchanger and is then expanded in the sweep gas turboexpander to recover useful power from the stream. The steam/O<sub>2</sub> stream is then sent through heat regenerator 1 before being exhausted to the surroundings.

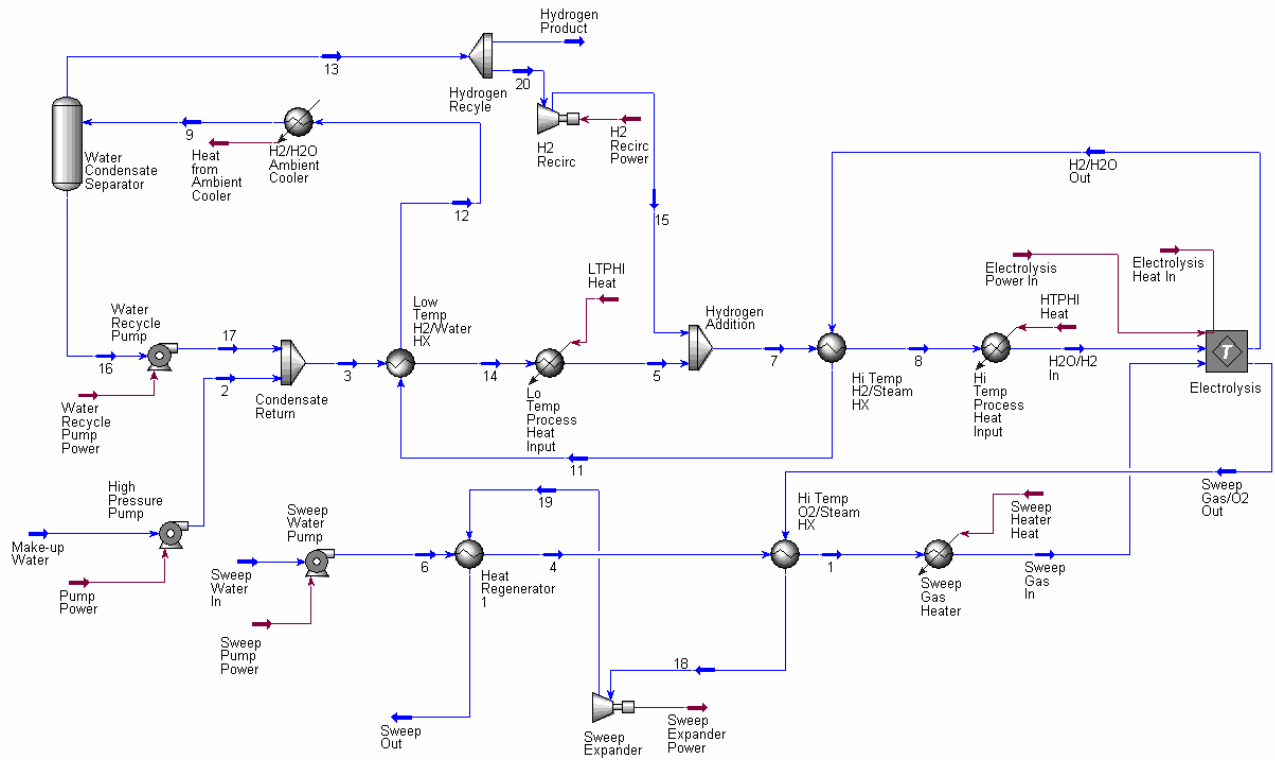


Figure 5. HYSYS process flow diagram for a 300 MW HTE plant with steam sweep.

The process flow diagram developed for the no-sweep case is shown in Fig. 6. For this case, the electrolysis stack would include only a single gas inlet stream (steam/hydrogen) and two gas outlet streams (hydrogen/steam and oxygen). A sweep gas inlet is shown in Fig. 6, but its flow rate is set to zero. Since the electrolysis cell produces oxygen, rather than consuming it as in the fuel-cell mode, a sweep gas stream is not necessarily required. There has been some discussion of the possible need for a sweeping flow of air or steam to dilute the oxygen in order to avoid possible materials and safety issues related to handling of pure oxygen at temperatures over 800°C. From a thermodynamic efficiency standpoint, the use of a non-oxygen-containing sweep gas improves the electrolyzer efficiency, but there are also some disadvantages associated with the use of an air sweep. First, dilution of the pure oxygen that is produced in the electrolysis stack with air would be wasteful since pure oxygen is a valuable commodity that could be sold as an electrolysis by-product. Second, production of a sweeping flow of high-pressure air at even a modest flow rate requires a significant amount of compressor power, compared to the electrolysis stack power consumption, which would seriously degrade the overall process efficiency, if a corresponding outlet turboexpander is not used. Finally, our research has indicated that pure oxygen can be safely handled at high temperature, if the right materials are used. Possible materials for this application include inconel alloys with dispersed aluminum and niobium-55 titanium alloys.

The flow diagram for the no-sweep case is very similar to the air-sweep case, but this flow diagram is simpler. Compared to the air-sweep case, the sweep gas compressor, the high-temperature air/oxygen heat exchanger, and the sweep gas heater are all eliminated, otherwise the diagrams are identical.

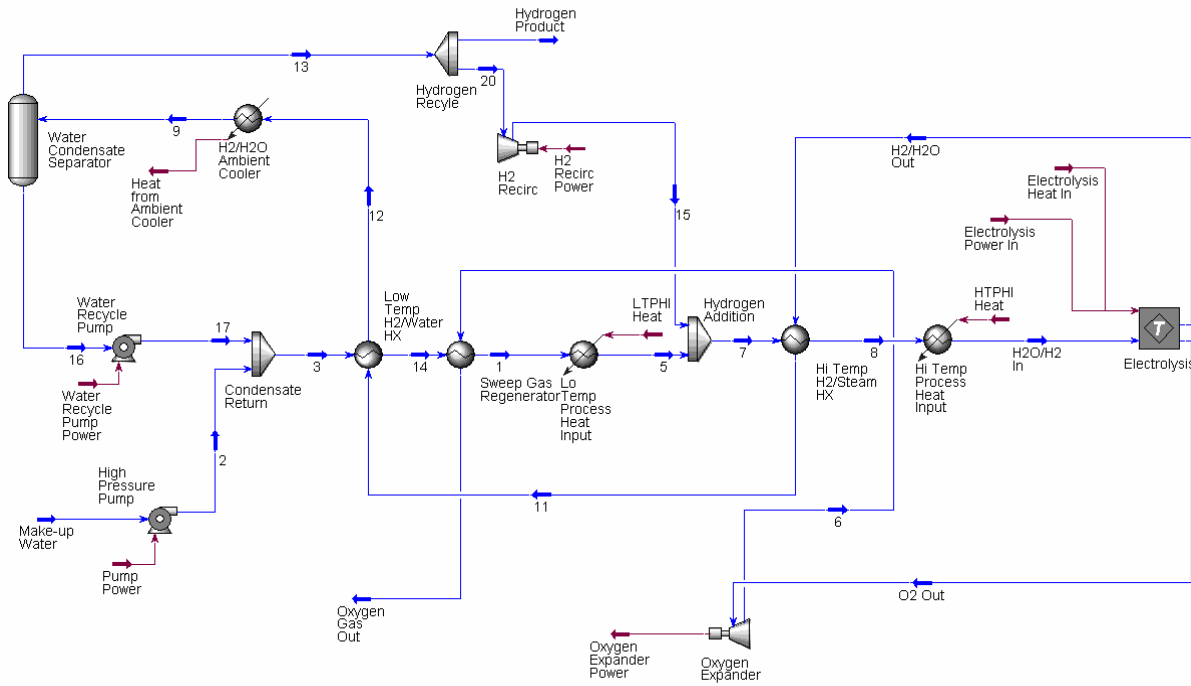


Figure 6. HYSYS process flow diagram for a 300 MW HTE plant with no sweep.

## RESULTS OF PARAMETRIC STUDIES ON A 300 MW HTE PLANT

A summary of the cases that have been studied is provided in Table 1. The second column in the table designates the sweep gas condition: air sweep, steam sweep, or no sweep. The third column designates the electrolyzer thermal boundary condition: isothermal or adiabatic. Isothermal operation requires direct heating of the electrolyzer by some means. The fourth column designates the per-cell ASR of the electrolyzer stack at a temperature of 1100 K. The ASR value used in the electrolyzer module is temperature- dependent per the following Arrhenius equation:

$$ASR(T) = ASR_{1100K} - 0.463 + 3.973 \times 10^{-5} \exp\left(\frac{10300}{T(K)}\right) \quad (11)$$

where  $ASR_{1100K}$  represents the user-specified cell ASR at the temperature 1100 K. This constant allows one to shift the entire ASR curve to higher or lower ASR values, to mimic lower or higher performing cells, respectively. This equation for  $ASR(T)$  is based on empirical data obtained from an actual operating stack, modified to allow user specification of the ASR value at 1100 K. In order to show the trends that can be expected with higher or lower ASR, two values of  $ASR_{1100K}$  have been included in this study. The  $ASR_{1100K}$  value of 1.25 represents a stack-average ASR value at 1100 K that should be achievable in the short term with existing technology. The  $ASR_{1100K}$  value of 0.25 is an optimistic value that has been observed in button cells, but will be difficult to achieve in a stack in the short term. The temperature dependence of the ASR is important for the adiabatic cases (since the outlet temperature in these cases is generally different than the inlet temperature) and for evaluating the effect of electrolyzer inlet temperature on overall process efficiency.

**Table 1.** Matrix of HYSYS test cases analyzed.

Case #	Sweep Gas	Electrolyzer Thermal BC	ASR at 1100 K	Steam Utilization	Inlet Temp (K)	P (MPa)
1	air	isothermal	1.25	fixed	1100	5
2	air	isothermal	0.25	fixed	1100	5
3	air	adiabatic	1.25	fixed	1100	5
4	air	adiabatic	0.25	fixed	1100	5
5	steam	isothermal	1.25	fixed	1100	5
6	steam	isothermal	0.25	fixed	1100	5
7	steam	adiabatic	1.25	fixed	1100	5
8	steam	adiabatic	0.25	fixed	1100	5
9	none	isothermal	1.25	fixed	1100	5
10	none	isothermal	0.25	fixed	1100	5
11	none	adiabatic	1.25	fixed	1100	5
12	none	adiabatic	0.25	fixed	1100	5
13	none	isothermal	0.25	variable, high flow rate	1100	5
14	none	isothermal	1.25	variable, low flow rate	1100	5
15	none	adiabatic	0.25	variable, high flow rate	1100	5
16	none	adiabatic	1.25	variable, low flow rate	1100	5
17	none	isothermal	0.25	fixed	1100-1200	5
18	none	isothermal	1.25	fixed	1100-1200	5
19	none	adiabatic	0.25	fixed	1100-1200	5
20	none	adiabatic	1.25	fixed	1100-1200	5

The fifth column in Table 1 designates the steam utilization condition: fixed or variable. All cases studied have an inlet steam composition of 95%, with 5% hydrogen. Fixed steam utilization cases have an outlet steam composition of 5%, and 95% hydrogen. For this case of fixed inlet and outlet compositions, the allowable inlet flow rate per cell of steam and hydrogen is dependent upon the current density and both must be varied simultaneously. The sweep gas flow rate is similarly scaled in each case. We have also run some cases with fixed inlet flow rate and composition, over a range of current densities. In these cases, the outlet steam composition will vary. These are the variable steam utilization cases. For low ASR values, higher current densities are achievable and a higher flow rate is needed to avoid steam starvation in the range of operating voltages of interest (up to the thermal neutral voltage).

Column 6 in Table 1 specifies the electrolyzer feed inlet temperature. Most cases used an inlet temperature of 1100 K. However, several cases were assessed for electrolyzer inlet temperatures of 1150 K and 1200 K. The electrolyzer operating pressure and the final hydrogen product delivery pressure for all cases was 5 MPa.

Results obtained from the HYSYS simulations are presented in Figs. 7 – 11. For these figures, filled symbols represent adiabatic electrolyzer operation, and open symbols represent isothermal operation. We are presenting primarily the overall thermal-to-hydrogen efficiency results, calculated using Eqn. (5). The HYSYS model also provides many additional details on process conditions at numerous locations around the process loop. Various process flow schemes and intermediate temperatures were studied to optimize the overall process

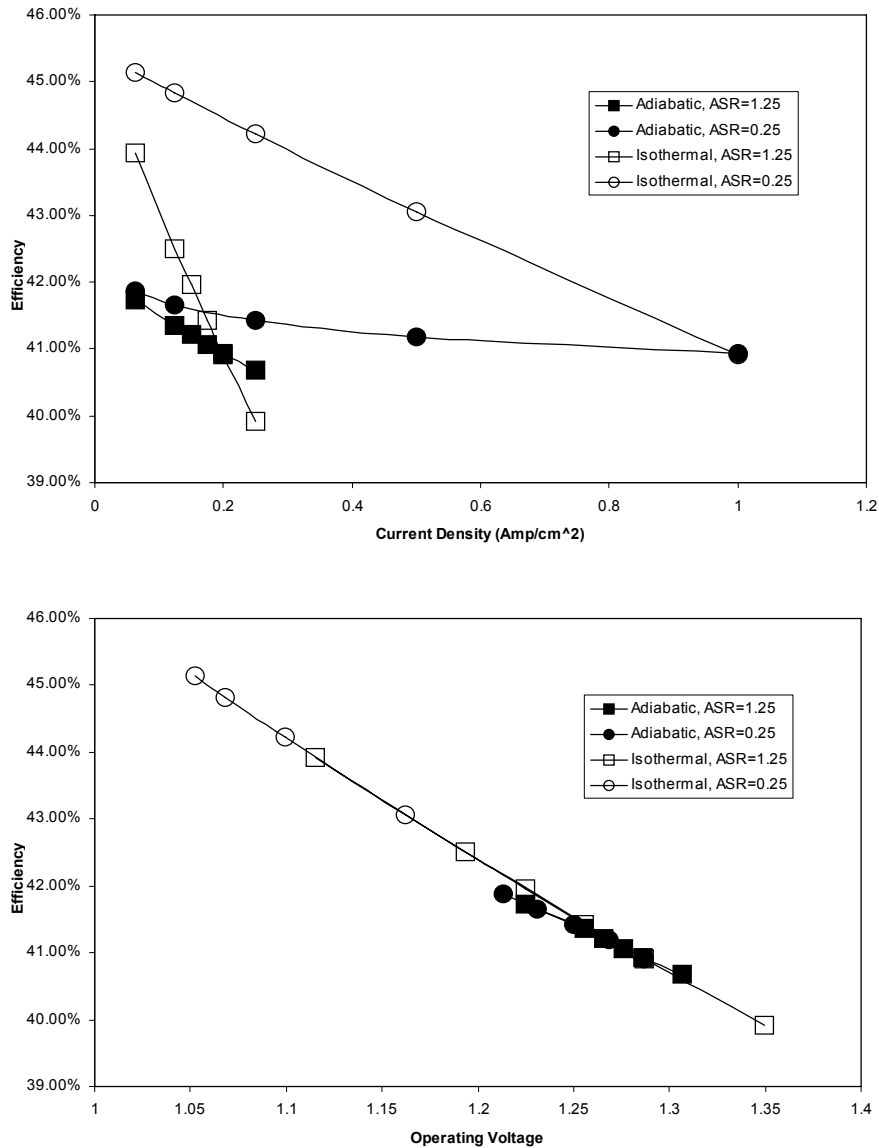


Figure 7. Overall thermal-to-hydrogen efficiencies (LHV) for Cases 1 – 4 (air sweep, fixed steam utilization, 1100 K electrolyzer inlet temperature, 5 MPa).

efficiency. We anticipate that some further improvement in overall thermal-to-hydrogen efficiency can still be achieved via process flow modifications.

Overall thermal-to-hydrogen efficiencies are presented in Fig. 7 as a function of electrolyzer current density and operating voltage for Cases 1 – 4 in Table 1. Note that current density is directly proportional to the hydrogen production rate, in accordance with Eqn. (2). The current density range for each case runs from a minimum value of 0.0625 A/cm<sup>2</sup> to a maximum value that depends on ASR. The maximum current density value for each case was selected to yield an operating voltage near or slightly above the thermal neutral voltage. For our analyses, the per-cell active area was assumed to be 225 cm<sup>2</sup> (15 cm x 15 cm) and the number of cells was fixed at  $3.994 \times 10^6$ . This cell area and number of cells yields 300 MW of hydrogen production (based on LHV) for Case 1 of Table 1 at a current density of 0.25 A/cm<sup>2</sup>.

For a specified *ASR* value and fixed steam utilization, lower current densities and the corresponding lower operating voltages yield higher overall efficiencies. Overall efficiencies plotted versus electrolyzer operating voltage tend to collapse onto a single curve, as expected. Note that at  $V_{op} = V_{tn}$  the electrolyzer overall thermal-to-hydrogen efficiency given by Eqn (8) would be the same as the power cycle efficiency (45%). The process overall thermal-to-hydrogen efficiency predicted from the process model is lower, however, due to incomplete heat recuperation of the sweep and steam streams, heat exchanger inefficiencies, and piping pressure losses. At the lowest current densities (and operating voltages) the thermal-to-hydrogen conversion efficiencies did exceed the power cycle efficiency. Overall trends indicate that isothermal electrolyzer operation is favorable over adiabatic, due to higher average electrolyte operating temperatures (and resulting lower *ASR* – Equation 11). Also, the rate of efficiency degradation as a function of current density is greater for higher *ASR* electrolyzers.

Fig. 8 presents the thermal-to-hydrogen efficiency results for steam sweep Cases 5 – 8. Trends are similar to those for an air sweep. Surprisingly, from an overall process efficiency standpoint, the steam sweep cases resulted in slightly lower performance than the corresponding air sweeps. As explained above, for electrolysis, it is desirable to have as low of a Nernst potential as possible, since the operating cell current density is proportional to the difference between the operating voltage and the Nernst potential (Equation 10). On the steam/hydrogen side of the electrolysis cell, the use of high inlet steam mole fraction and a high total steam flow rate is desirable. On the oxygen side, a low average oxygen mole fraction is desirable. Therefore, focusing only on the electrolyzer, a non-oxygen-containing sweep gas such as steam should lead to a higher efficiency than a sweep gas such as air. This would apply to the entire process as well if total heat recuperation were possible. However, the final exhaust temperature of the oxygen-laden steam sweep was approximately 350 K -- it was not possible to recover more from this “low-quality heat” stream in spite of the fact that it still contains significant latent and sensible heat.

The thermal-to-hydrogen efficiency results for the case of no sweep gas are presented in Fig. 9. These cases exhibited overall thermal-to-hydrogen efficiencies as high as 46%, higher than the power-cycle efficiency. Recall that this overall efficiency accounts for electrolysis irreversibilities, heat transfer inefficiencies, incomplete heat recuperation, and pumping losses. This important result supports the earlier theoretical discussion that the overall thermal-to-hydrogen efficiency can exceed the power-cycle efficiency under certain circumstances.

For cases 1-12, the  $H_2O / H_2$  feed flow rate was allowed to vary and the percentage steam utilization was fixed. The effects of allowing the percentage utilization to vary for a fixed inlet mass flow rate are displayed in Fig 10 for various current densities and corresponding operating voltages. The mass flow rate used for these cases was large enough to prevent steam starvation at the highest current density value used for each *ASR* value. These results are quite different than the fixed utilization results. The overall efficiencies for these cases actually tend to increase with increasing current density. Also, the efficiencies for the four voltage sweeps (adiabatic vs. isothermal, 1.25 *ASR* vs. 0.25 *ASR*) do not collapse onto a single line, as did the fixed utilization cases. Furthermore, for the range of current densities and voltages considered, the isothermal cases exhibited a maximum efficiency at an

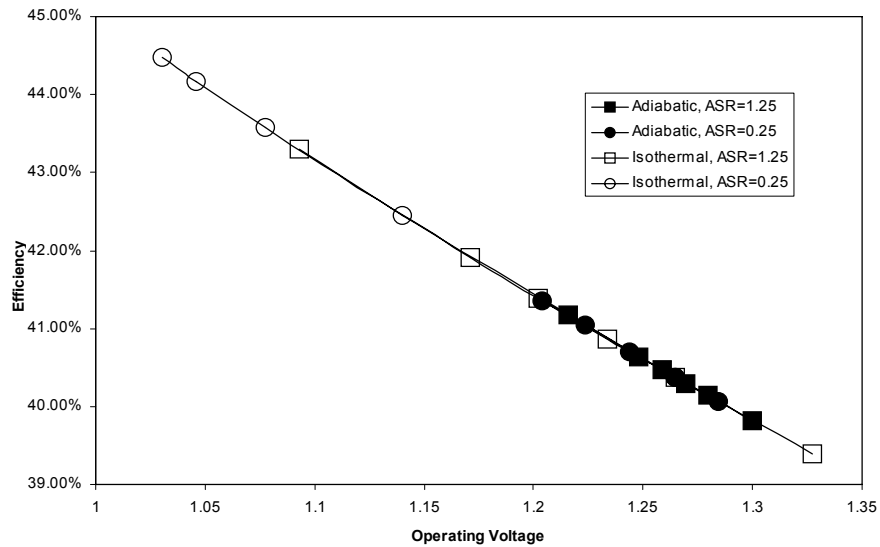
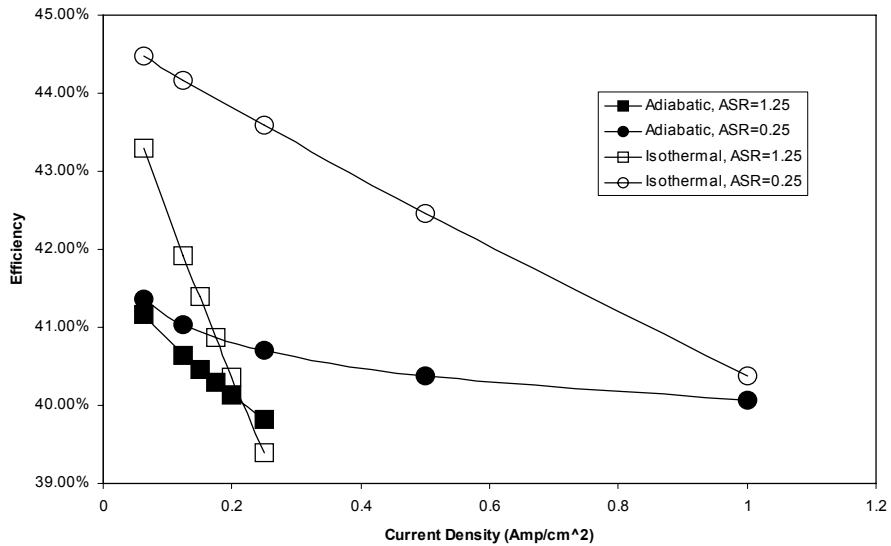


Figure 8. Overall thermal-to-hydrogen efficiencies (LHV) for Cases 5 – 8 (steam sweep, fixed steam utilization, 1100 K electrolyzer inlet temperature, 5 MPa).

intermediate current density. For the low-current-density cases, the fixed mass-flow constraint yields poorer heat recuperation, due to the presence of considerable excess steam.

Purely from the standpoint of electrolyzer efficiency, the presence of excess steam should yield higher efficiency, but the problem is with the inability to fully recuperate heat from the exiting excess steam. As the current density and steam utilization are increased, the overall process efficiency achieves a maximum value, where the thermodynamic benefit of the excess steam (lower Nernst potential) outweighs the heat recuperation issue.

The effects of electrolyzer operating temperature on overall system performance, with fixed steam utilization, at a current density of 0.25, are shown in Fig. 11. As expected, overall hydrogen production efficiency increases with increasing electrolyzer temperature. Efficiencies for isothermal operation demonstrate the highest temperature dependency. The overall

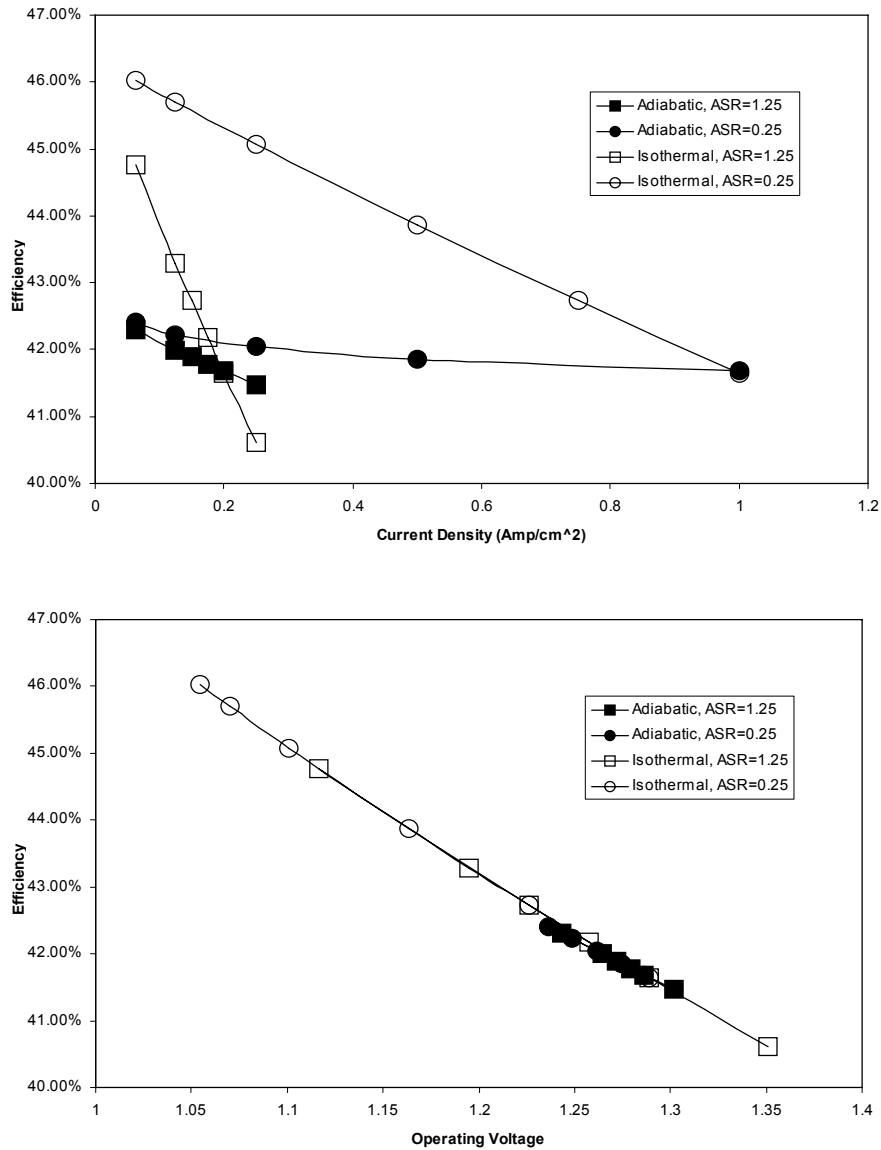


Figure 9. Overall thermal-to-hydrogen efficiencies (LHV) for Cases 9 – 12 (no sweep, fixed steam utilization, 1100 K electrolyzer inlet temperature, 5 MPa).

process efficiency for  $ASR_{1100K} = 0.25$  and an isothermal electrolyzer approaches 47% at 1200 K inlet temperature. Electrolyzer outlet temperatures are plotted versus electrolyzer inlet temperature in the bottom graph of Fig. 11. Electrolyzer outlet temperatures depend strongly upon the ASR value and its temperature dependence (extent of ohmic heating). Outlet temperatures for the lower ASR simulations remained below the corresponding inlet temperature. The outlet temperatures for higher ASR simulations displayed more complicated behavior, remaining higher than inlet temperatures up to approximately 1160 K inlet.

## SUMMARY AND CONCLUSIONS

An engineering process model for a large-scale 300 MW High-Temperature Electrolysis H<sub>2</sub> production facility has been developed at the INL. This model links an INL-developed one-dimensional electrolyzer model within the commercial HYSYS code. Detailed process flowsheets have been defined that include all of the components that would be

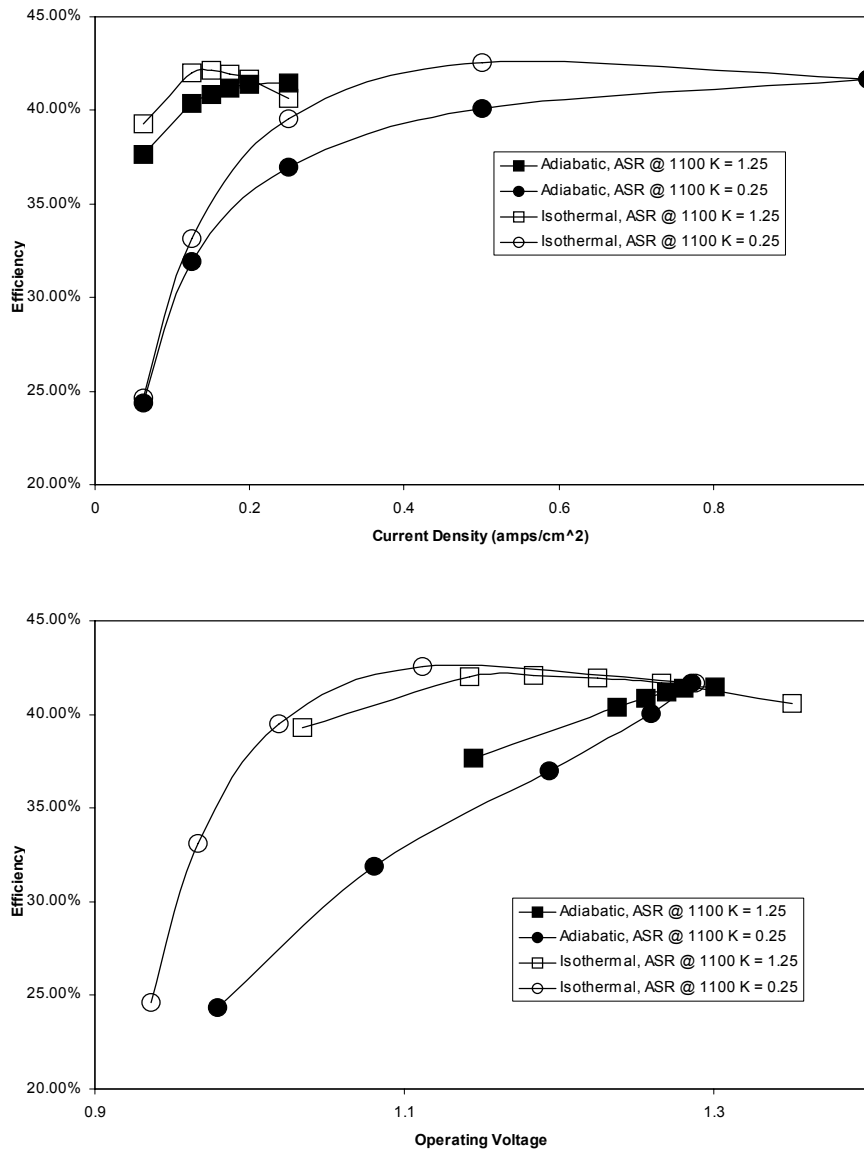


Figure 10. Overall thermal-to-hydrogen efficiencies (LHV) for Cases 13 – 16 (no sweep, fixed electrolyzer feed flowrate, 5 MPa).

present in an actual plant such as pumps, compressors, heat exchangers, turbines, and the electrolyzer. The electrolyzer model allows for the determination of the operating voltage, gas outlet temperatures, and electrolyzer efficiency for any specified inlet gas flow rates/compositions, current density, cell active area, and external heat loss or gain.

The one-dimensional electrolyzer model was validated by comparison with results obtained from a fully 3-D computational fluid dynamics model developed using FLUENT. Process modeling results indicate that overall thermal-to-hydrogen efficiencies based upon LHV can exceed the power-cycle (electrical production) efficiency. Thermodynamic evaluation of the electrolyzer alone indicates that minimizing the Nernst voltage through use of a steam sweep would maximize production efficiency. This was not the case when the overall process was evaluated. Unfortunately, loss of some “low quality” heat through the sweep gas is unavoidable. In fact, the use of a steam sweep yielded lower performance than the use of an

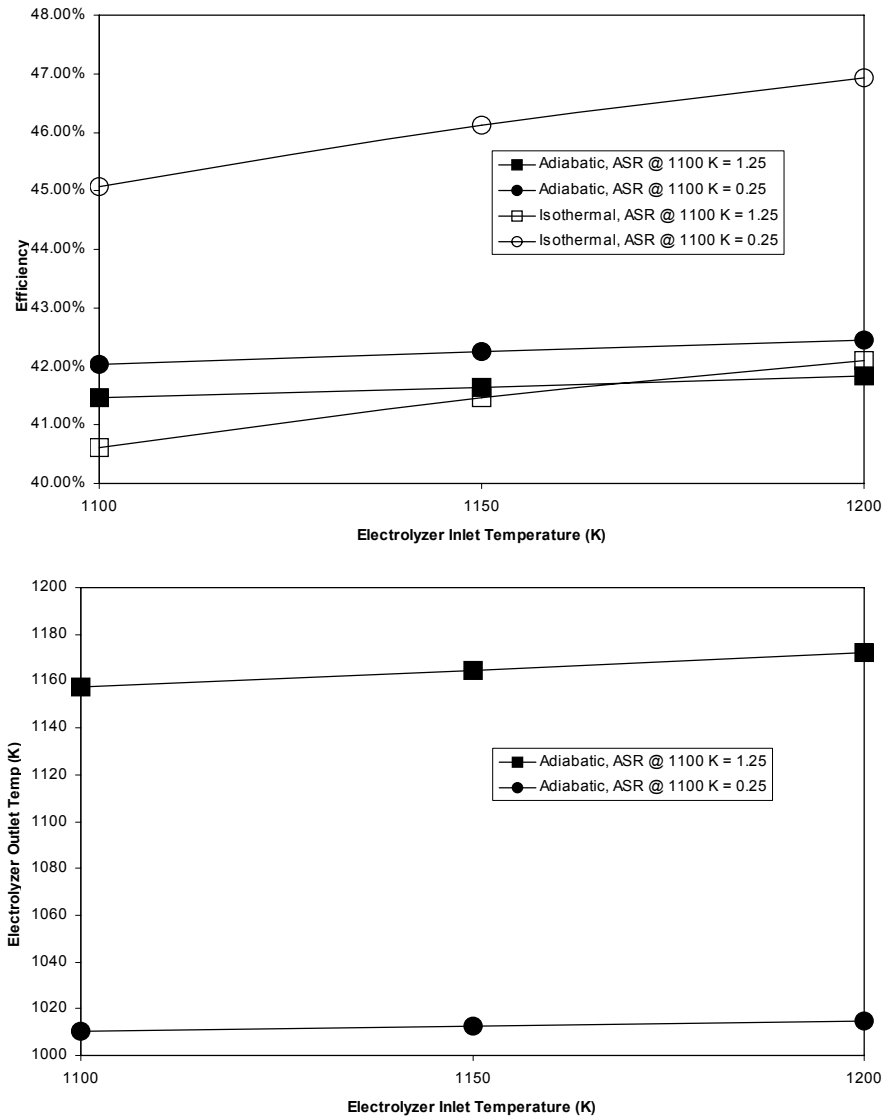


Figure 11. Overall thermal-to-hydrogen efficiencies (LHV) and electrolyzer outlet temperatures for Cases 17 – 20 (no sweep, fixed steam utilization, fixed current density of 0.25 A/cm<sup>2</sup>, 5 MPa).

air sweep. Overall process efficiencies favored the use of no sweep gas, despite the high oxygen composition.

Isothermal electrolyzer operation was preferable over adiabatic due to higher average cell temperatures and corresponding lower ASR values. The temperature dependence of ASR favored operation of the electrolyzer at as high a temperature as possible. For a fixed inlet flow rate, the degree of steam utilization within the electrolyzer also had an effect upon overall process efficiency. Overall process efficiency generally improves with increasing steam utilization. However, to prevent damage to the electrolyzer, steam utilization should be kept somewhat below 100% (e.g., 95%) to avoid steam starvation.

## REFERENCES

1. O'Brien, J. E., Stoots, C. M., Herring, J. S., and Hartvigsen, J. J., "Hydrogen Production Performance of a 10-Cell Planar Solid-Oxide Electrolysis Stack," Proceedings, ASME 3rd International Conference on Fuel Cell Science, Engineering, and Technology, May 23 – 25, 2005, Ypsilanti, MI.
2. O'Brien, J. E., Herring, J. S., Stoots, C. M., Lessing, P. A., "High-Temperature Electrolysis for Hydrogen Production From Nuclear Energy," 11<sup>th</sup> International Topical Meeting on Nuclear Reactor Thermal-Hydraulics NURETH-11, Popes Palace Conference Center, Avignon, France, October 2-6, 2005.
3. O'Brien, J. E., Stoots, C. M., Herring, J.S., Lessing, P. A., Hartvigsen, J. J., and Elangovan, S., "Performance Measurements of Solid-Oxide Electrolysis Cells for Hydrogen Production from Nuclear Energy," *Journal of Fuel Cell Science and Technology*, Vol. 3, August 2005, pp. 72-82.
4. Hawkes, G. L., O'Brien, J. E., Stoots, C. M., Herring, J. S., Shahnam, M., "CFD Model of a Planar Solid Oxide Electrolysis Cell for Hydrogen Production from Nuclear Energy," 11th International Topical Meeting on Nuclear Reactor Thermal-Hydraulics NURETH-11, Popes Palace Conference Center, Avignon, France, October 2-6, 2005.
5. Hawkes, G. L., O'Brien, J. E., Stoots, C. M., Herring, J. S., Shahnam, M., "Thermal and Electrochemical Three Dimensional CFD Model of a Planar Solid Oxide Electrolysis Cell," 2005 ASME Heat Transfer Conference, July 17-22, 2005, San Francisco.
6. O'Brien, J. E., Stoots, C. M., and Hawkes, G. L., "Comparison of a One-Dimensional Model of a High-Temperature Solid-Oxide Electrolysis Stack with CFD and Experimental Results," to be published in the Proceedings of 2005 ASME International Mechanical Engineering Congress and Exposition IMECE2005, Orlando, Florida, November 5-11, 2005.
7. Yildiz, B., and Kazimi, M. S., "Nuclear Energy Options for Hydrogen and Hydrogen-Based Liquid Fuels Production," MIT-NES-TR-001, September 2003.